Received: 14 May 2019 | Revised: 8 December 2019 | Accepted: 21 December 2019

DOI: 10.1111/cas.14301

ORIGINAL ARTICLE

Cancer Science WILEY

Solid-type poorly differentiated adenocarcinoma of the stomach: Deficiency of mismatch repair and SWI/SNF complex

Shinichi Tsuruta[1] | Kenichi Kohashi[1] | Yuichi Yamada[1] | Minako Fujiwara[1] | Yutaka Koga[1] | Eikichi Ihara[2] | Yoshihiro Ogawa[2] | Eiji Oki[3] | Masafumi Nakamura[4] | Yoshinao Oda[1]

[1]Department of Anatomic Pathology, Graduate School of Medical Sciences, Kyushu University, Fukuoka, Japan

[2]Department of Medicine and Bioregulatory Science, Graduate School of Medical Sciences, Kyushu University, Fukuoka, Japan

[3]Department of Surgery and Science, Graduate School of Medical Sciences, Kyushu University, Fukuoka, Japan

[4]Department of Surgery and Oncology, Graduate School of Medical Sciences, Kyushu University, Fukuoka, Japan

Correspondence
Yoshinao Oda, Department of Anatomic Pathology, Pathological Sciences, Graduate School of Medical Sciences, Kyushu University, Fukuoka, Japan.
Email: oda@surgpath.med.kyushu-u.ac.jp

Abstract

ARID1A, one of the subunits in SWI/SNF chromatin remodeling complex, is frequently mutated in gastric cancers with microsatellite instability (MSI). The most frequent MSI in solid-type poorly differentiated adenocarcinoma (PDA) has been reported, but the SWI/SNF complex status in solid-type PDA is still largely unknown. We retrospectively analyzed 54 cases of solid-type PDA for the expressions of mismatch repair (MMR) proteins (MLH1, PMS2, MSH2, and MSH6), SWI/SNF complex subunits (ARID1A, INI1, BRG1, BRM, BAF155, and BAF170) and EBER, and mutations in *KRAS* and *BRAF*. We analyzed 40 cases of another histological type of gastric cancer as a control group. The solid-type PDAs showed coexisting glandular components (76%), MMR deficiency (39%), and complete/partial loss of ARID1A (31%/7%), INI1 (4%/4%), BRG1 (48%/30%), BRM (33%/33%), BAF155 (13%/41%), and BAF170 (6%/2%), EBER positivity (4%), *KRAS* mutation (2%), and *BRAF* mutation (2%). Compared to the control group, MMR deficiency and losses of ARID1A, BRG1, BRM, and BAF155 were significantly frequent in solid-type PDAs. Mismatch repair deficiency was associated with the losses of ARID1A, BRG1, and BAF155 in solid-type PDAs. In the MMR-deficient group, solid components showed significantly more frequent losses of ARID1A, BRG1, BRM, and BAF155 compared to glandular components (P = .0268, P = .0181, P = .0224, and P = .0071, respectively). In the MMR-proficient group, solid components showed significantly more frequent loss of BRG1 compared to glandular components (P = .012). In conclusion, solid-type PDAs showed frequent losses of MMR proteins and the SWI/SNF complex. We suggest that loss of the SWI/SNF complex could induce a morphological shift from differentiated-type adenocarcinoma to solid-type PDA.

KEYWORDS

gastric cancer, mismatch repair, poorly differentiated adenocarcinoma, solid carcinoma, SWI/SNF complex

Abbreviations: EBV, Epstein-Barr virus; EBVaGC, EBV-associated GC; GC, gastric cancer; GS, genomically stable; MC, medullary carcinoma; MMR, mismatch repair; MSI, microsatellite instability; PDA, poorly differentiated adenocarcinoma; QMVR, quasimonomorphic variation range; TIL, tumor-infiltrating lymphocyte.

1 | INTRODUCTION

Gastric cancer remains the third leading cause of cancer death worldwide. Although it is commonly supposed that PDA has a worse prognosis than other histological types, several studies showed that PDA with solid morphology is associated with a favorable prognosis despite its poorly differentiated histology.[1-4] According to the Japanese classification, PDAs are divided into the solid-type and nonsolid-type.[5]

Solid-type PDAs often contain a glandular component that tends to be detected superficially in the tumor, suggesting that solid-type PDAs develop from a tubular or papillary adenocarcinoma.[6] Previous studies reported that solid-type PDA is associated with MSI,[6,7] which is caused by inactivation of MMR proteins such as MLH1, PMS2, MSH2, and MSH6.

A close relationship has been identified between MSI and ARID1A alteration in some neoplasms.[8-15] SWI/SNF family members such as ARID1A, INI1, BRG1, BRM, BAF155, and BAF170 are involved in the regulation of vital cellular processes, such as proliferation and differentiation, in a wide variety of neoplasms.[16-19] However, no analysis of the expression status of SWI/SNF family members in solid-type PDAs has been undertaken to date.

In this study, we investigated the expression status of MMR proteins and SWI/SNF complex subunits by using samples from patients with solid-type PDAs, and we compared the immunohistochemical status of the PDAs' glandular components and solid components. We undertook this investigation to elucidate the clinicopathological and molecular biological characteristics of solid-type PDAs of the stomach.

2 | MATERIALS AND METHODS

2.1 | Case selection

A total of 1810 cases of GC were resected at Kyushu University Hospital (Fukuoka, Japan) and affiliated hospitals from 2006 to 2012. Using the surgical pathology files of Kyushu University Hospital, we collected 54 GC cases (54/1810, 3.0%) diagnosed as solid-type PDA. According to the Japanese Classification of Gastric Carcinoma,[5] solid-type PDA shows a sheet-like solid growth pattern with scanty stroma (Figure 1). Special histological types such as lymphoepithelioma-like carcinomas, neuroendocrine carcinoma, and hepatoid adenocarcinoma were excluded. Additionally, we selected 40 cases of stage-matched GC without solid-type PDA as a control group, whose time of receiving gastrectomy was close to that of the solid-type PDA groups. All patients were staged according to the 8th edition of the UICC TNM classification. In a control group, 25 of 40 cases were tubular adenocarcinomas, and 15 of 40 cases were nonsolid-type PDAs or signet-ring cell carcinomas. None of cases received preoperative chemotherapy except for 1 case of solid-type PDA. All of the patients had undergone curative resection. The research protocol was approved by the Kyushu University Medical Human Investigation Committee (Institutional Review Board no. 29-240).

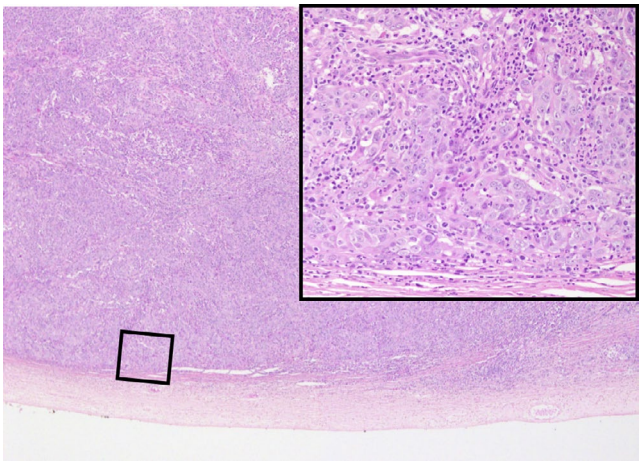

FIGURE 1 Solid-type poorly differentiated adenocarcinoma showing an expansive growth pattern at the periphery. High-magnification image (200×) showing tumor-infiltrating lymphocytes and tumor cells with vesicular nuclei and prominent nucleoli

2.2 | Clinicopathological assessment

We analyzed the clinical characteristics of all cases, including patient age, sex, tumor location, tumor size, growth pattern, lymphatic and venous invasion, coexisting glandular component, TILs, Crohn's-like reaction, and the UICC TNM stage. Tumor-infiltrating lymphocytes and Crohn's-like reaction were evaluated as described.[20,21]

2.3 | Immunohistochemistry

We undertook immunohistochemical staining using the universal immunoperoxidase polymer method (EnVision Kit; Dako) or the streptavidin-biotin-peroxidase method (Histofine) for all available cases. Formalin-fixed, paraffin-embedded tissues were sectioned at 4 μm. Antigen retrieval was carried out by boiling the slides with 10 mM sodium citrate (pH 6.0) or Target Retrieval Solution (Dako). The primary Abs and staining conditions are summarized in Table 1.

The expressions of MMR proteins (MLH1, PMS2, MSH2, and MSH6) were judged as "loss" when there was a complete absence of nuclear staining in neoplastic cells, while the surrounding nonneoplastic cells showed consistently preserved nuclear staining.

In our assessment of ARID1A, INI1, BRM, BRG1, BAF155, and BAF170, only unequivocally clearly absent staining in the nuclei of viable tumor tissue (away from necrotic areas) was considered "loss." As a control, the presence of homogenous strong nuclear staining of stromal fibroblasts, inflammatory cells, vascular endothelial cells, or normal epithelial cells in the background was a prerequisite for assessable staining in the tumor. Staining proportion was graded

TABLE 1 Primary Abs used for immunohistochemical staining

Antibody	Clone	Company	Dilution
MLH1	G168-15	BD Bioscience	1:50
PMS2	A16-4	BD Bioscience	1:200
MSH2	Ab-2	Calbiochem	1:100
MSH6	EP49	Dako	1:200
ARID1A	Polyclonal	SIGMA	1:500
SMARCB1/INI1	25/BAF47	BD Bioscience	1:250
SMARCA4/BRG1	G-7	Santa Cruz Biotechnology	1:25
SMARCA2/BRM	Polyclonal	Abcam	1:50
SMARCC1/BAF155	DXD7	Santa Cruz Biotechnology	1:50
SMARCC2/BAF170	E-6	Santa Cruz Biotechnology	1:100

as complete loss (0%-4%), partial loss (5%-49%), or retained (50%-100%) based on a described labeling index.[22]

2.4 | In situ hybridization of EBV-encoded small RNA (EBER)

To examine the EBV infection status, we stained 3-μm-thick sections for in situ hybridization. EBER probe (#Y5200; Dako) was detected using the PNA ISH Detection Kit (#K5201; Dako). Identifiable nuclear staining for EBER was interpreted as a positive result.

2.5 | Mutational analysis

We carried out PCR and a Sanger sequencing analysis to detect gene mutations in *KRAS* codons 12 and 13, and *BRAF* (V600E). Genomic DNA was extracted from paraffin-embedded tissue using a QIAamp DNA FFPE Tissue Kit (Qiagen) according to the manufacturer's instructions. The PCR conditions and primer sequences as well as the Sanger sequence procedures were as described.[23] If the quality of the DNA or the level of PCR amplification in a patient's case was insufficient for a mutation analysis, the case was excluded from the molecular study.

2.6 | Microsatellite instability analysis

Microsatellite instability analysis was carried out by using an MSI Analysis Kit (FALCO) (FALCO Biosystems) with the 5 microsatellite markers BAT-26, NR-21, BAT-25, MONO-27, and NR-24, according to the QMVR method without paired normal DNA reported previously.[24] The PCR was carried out using the Veriti thermal cycler (Life Technologies), and PCR amplicon was diluted by distilled water and applied to a 3130xl Genetic Analyzer (Life Technologies). Fragment analysis was undertaken by GeneMapper software (Life Technologies). Tumors showing markers outside the corresponding QMVR were defined as MSI. We classified the tumors as MSI-High if 2 or more of the 5 markers showed MSI, and negative (MSI-Low or MSS) if one marker or less showed MSI.

2.7 | Statistical analysis

We assessed statistical differences between the groups using the Mann-Whitney *U* test, the χ^2 test, or Fisher's exact test. Survival data were assessed by the Kaplan-Meier method and tested for significance between the groups with the log-rank test. All calculations were undertaken using JMP software version 13.0 (SAS Institute). *P* values less than .05 were considered significant.

3 | RESULTS

3.1 | Clinicopathological status, immunohistochemistry, and in situ hybridization

The clinicopathological features and results of immunohistochemistry and in situ hybridization are summarized in Tables 2 and 3, and representative immunohistochemical images are provided in Figure 2. Of the patients with solid-type PDAs, 35 were men and 19 were women, with a median age of 74.5 years (range, 55-90 years). Solid-type PDAs showed frequent expansive growth patterns (52%), TILs (57%), Crohn's-like reaction (33%), and coexisting glandular component (76%). Mismatch repair deficiency was seen in 21 of the 54 tumors (39%). All of the MMR-deficient tumors showed a concurrent loss of MLH1/PMS2, and none of the cases showed other patterns of MMR deficiency. EBER positivity was found in 2 of the 54 cases (4%). The features of both EBER-positive tumors were male sex, TILs, upper-third location, and MMR proficient.

Solid components in solid-type PDAs are usually seen at the invasive area, whereas glandular components are seen at the superficial area. We evaluated the immunohistochemical status of solid components in solid-type PDAs and invasive areas of GC in the control group. The solid-type PDAs showed a complete/partial loss of ARID1A (31%/7%), INI1 (4%/4%), BRG1 (48%/30%), BRM (33%/33%), BAF155 (13%/41%), and BAF170 (6%/2%). Compared to the control group, solid-type PDAs were associated with lower third location ($P = .0128$), larger size ($P = .0002$), expansive growth pattern ($P < .001$), TILs ($P < .001$), Crohn's-like reaction ($P = .0439$), MMR deficiency ($P = .0002$), and loss of ARID1A, BRG1, BRM, and BAF155 ($P = .0057$, $P < .001$, $P = .0005$, and $P = .0003$, respectively). In the control group, 15 cases of nonsolid-type PDA or signet-ring cell carcinoma showed a complete/partial loss of ARID1A (20%/0%), INI1 (0%/0%), BRG1 (0%/20%), BRM (7%/13%), BAF155 (20%/13%), and BAF170 (0%/0%), and 25 cases of tubular adenocarcinoma showed a complete/partial loss of ARID1A (4%/0%), INI1 (0%/0%), BRG1 (8%/20%), BRM (8%/24%), BAF155 (8%/0%), and BAF170 (0%/0%).

TABLE 2 Clinicopathologic status of solid-type poorly differentiated adenocarcinomas (PDAs) and gastric cancers in the control group

	Solid-type PDAs	Control group		MMR-deficient	MMR-proficient	
	n = 54	n = 40	*P* value	n = 21	n = 33	*P* value
Age, y; median (range)	74.5 (55-90)	69 (53-84)	.0026*	77 (62-90)	73 (55-87)	.1288
Male, n (%)	35 (65)	34 (85)	.0285*	9 (43)	26 (79)	.007*
Female, n (%)	19 (35)	4 (15)		12 (57)	7 (21)	
Location, n (%)						
U	10 (19)	14 (35)	.0128*	2 (10)	8 (24)	.0038*
M	23 (43)	21 (53)		5 (24)	18 (55)	
L	21 (39)	5 (13)		14 (67)	7 (21)	
Size, mm; median (range)	72 (12-170)	44 (15-140)	.0002*	74 (18-140)	70 (12-170)	.8521
Growth pattern, n (%)						
Expansile	28 (52)	4 (10)	<.001*	16 (76)	12 (36)	.0043*
Infiltrative	26 (48)	36 (90)		5 (24)	21 (64)	
Lymphatic invasion (+)	33 (61)	20 (50)	.2828	14 (67)	19 (58)	.5041
Venous invasion (+)	29 (54)	16 (40)	.1885	8 (38)	21 (64)	.0665
Tumor-infiltrating lymphocytes (+)	31 (57)	4 (10)	<.001*	21 (100)	10 (30)	<.001*
Crohn's-like reaction (+)	18 (33)	6 (15)	.0439	12 (57)	6 (18)	.0031*
Glandular component (+)	41 (76)	30 (75)	.9178	18 (86)	23 (70)	.1796
pT stage, n (%)						
pT1b-2	15 (28)	16 (40)	.2127	7 (33)	8 (24)	.4672
pT3-4	39 (72)	24 (60)		14 (67)	25 (76)	
pN stage, n (%)						
pN0	20 (37)	10 (25)	.2158	7 (33)	13 (39)	.653
pN1-3	34 (63)	30 (75)		14 (67)	20 (61)	
pM stage, n (%)						
M0	53 (98)	39 (98)	.8295	21 (100)	32 (97)	.4207
M1	1 (2)	1 (3)		0 (0)	1 (3)	
pStage, n (%)						
I	12 (22)	9 (23)	.997	6 (29)	6 (18)	.6836
II	18 (33)	13 (33)		6 (29)	12 (36)	
III	23 (43)	17 (43)		9 (43)	14 (42)	
IV	1 (2)	1 (3)		0 (0)	1 (3)	

Note: Data were analyzed using the χ^2 test, except for age and size, which were analyzed using the Mann-Whitney *U* test.
Abbreviations: L, lower third location; M, middle third location; MMR, mismatch repair; U, upper third location.
*Statistically significant.

Our comparison of the MMR-deficient and MMR-proficient groups revealed that the patients in the MMR-deficient group were relatively older than those in the MMR-proficient group (*P* = .1288). Mismatch repair deficiency was associated with female sex, lower third location, expansive growth pattern, TILs, and Crohn's-like reaction (*P* = .007, *P* = .0038, *P* = .0043, *P* < .001, and *P* = .0031, respectively). The MMR-deficient group showed significantly more frequent losses of ARID1A, BRG1, and BAF155 than the MMR-proficient group (*P* < .001, *P* = .0445, and *P* < .001, respectively). The MMR-deficient group showed more frequent losses of INI1, BRM, and BAF170 compared to the MMR-proficient group, but the differences were not significant (*P* = .1807, *P* = .7915, and *P* = .0631, respectively). All 21 of the MMR-deficient solid-type PDAs (100%) and 30 of the 33 MMR-proficient solid-type PDAs (91%) showed a complete or partial loss of at least 1 of the SWI/SNF complex subunits.

3.2 | Comparison of glandular and solid components: Immunohistochemical status of SWI/SNF complex components

Glandular components were seen in 18 of the 21 MMR-deficient tumors (86%) and 23 of the 33 MMR-proficient tumors (70%). We compared the immunohistochemical status of the glandular and

TABLE 3 Immunohistochemistry and in situ hybridization of solid-type poorly differentiated adenocarcinomas (PDAs) and gastric cancers in the control group

	Solid-type PDAs	Control group		MMR-deficient	MMR-proficient	
	n = 54; n (%)	n = 40; n (%)	*P* value	n = 21; n (%)	n = 33; n (%)	*P* value
Mismatch repair						
Deficient	21 (39)	2 (5)	.0002*			
Proficient	33 (61)	38 (95)				
EBER-ISH						
Positive	2 (4)	2 (5)	.7582	0 (0)	2 (6)	.2503
Negative	52 (96)	38 (95)		21 (100)	31 (94)	
ARID1A						
Complete loss	17 (31)	4 (10)	.0057*	14 (67)	3 (9)	<.001*
Partial loss	4 (7)	0 (0)		2 (10)	2 (6)	
Retained	33 (61)	36 (90)		5 (24)	28 (85)	
INI1						
Complete loss	2 (4)	0 0)	.2128	1 (5)	1 (3)	.1807
Partial loss	2 (4)	0 0)		2 (10)	0 (0)	
Retained	50 (93)	40 (100)		18 (86)	32 (97)	
BRG1						
Complete loss	26 (48)	2 (5)	<.001*	13 (62)	13 (40)	.0445*
Partial loss	16 (30)	8 (20)		7 (33)	9 (27)	
Retained	12 (22)	30 (75)		1 (5)	11 (33)	
BRM						
Complete loss	18 (33)	3 (8)	<.0005*	7 (33)	11 (33)	.7915
Partial loss	18 (33)	8 (20)		8 (38)	10 (30)	
Retained	18 (33)	29 (73)		6 (29)	12 (36)	
BAF155						
Complete loss	7 (13)	5 (13)	.0003*	6 (29)	1 (3)	<.001*
Partial loss	22 (41)	2 (5)		12 (57)	10 (30)	
Retained	25 (46)	33 (83)		3 (14)	22 (67)	
BAF170						
Complete loss	3 (6)	0 (0)	.2128	3 (14)	0 (0)	.0631
Partial loss	1 (2)	0 (0)		0 (0)	1 (3)	
Retained	50 (93)	40 (100)		18 (86)	32 (97)	

Note: Data were analyzed using the χ^2 test, except for age and size, which were analyzed using the Mann-Whitney *U* test.
Abbreviations: ISH, in situ hybridization; MMR, mismatch repair.
*Statistically significant.

solid components and observed that the expression pattern of MMR proteins was the same in both glandular and solid components in all cases. The features of the solid-type PDAs with glandular component are summarized in Table 4, and an example is presented in Figure 3. Loss of SWI/SNF family members was observed more frequently in solid components compared to the glandular components in both the MMR-deficient and -proficient groups.

In the MMR-deficient group, the differences in the expression status of ARID1A, BRG1, BRM, and BAF155 between the 2 types of components were significant (P = .0268, P = .0181, P = .0224, and P = .0071, respectively), but the differences in the expression status of INI1 and BAF170 did not reach significance (P = .3456 and P = .6299, respectively). In the MMR-proficient group, the difference in the expression status of BRG1 was significant (P = .012), but the differences in the expression status of ARID1A, INI1, BRM, BAF155, and BAF170 did not reach significance (P = .2966, P = .312, P = .3248, P = .3454, and P = .321, respectively).

3.3 | Molecular features

We analyzed the mutational status of *KRAS* and *BRAF* in solid-type PDAs. The results of the mutational analysis are summarized in Table 5. We excluded 13 and 12 tumors from the *KRAS* and *BRAF*

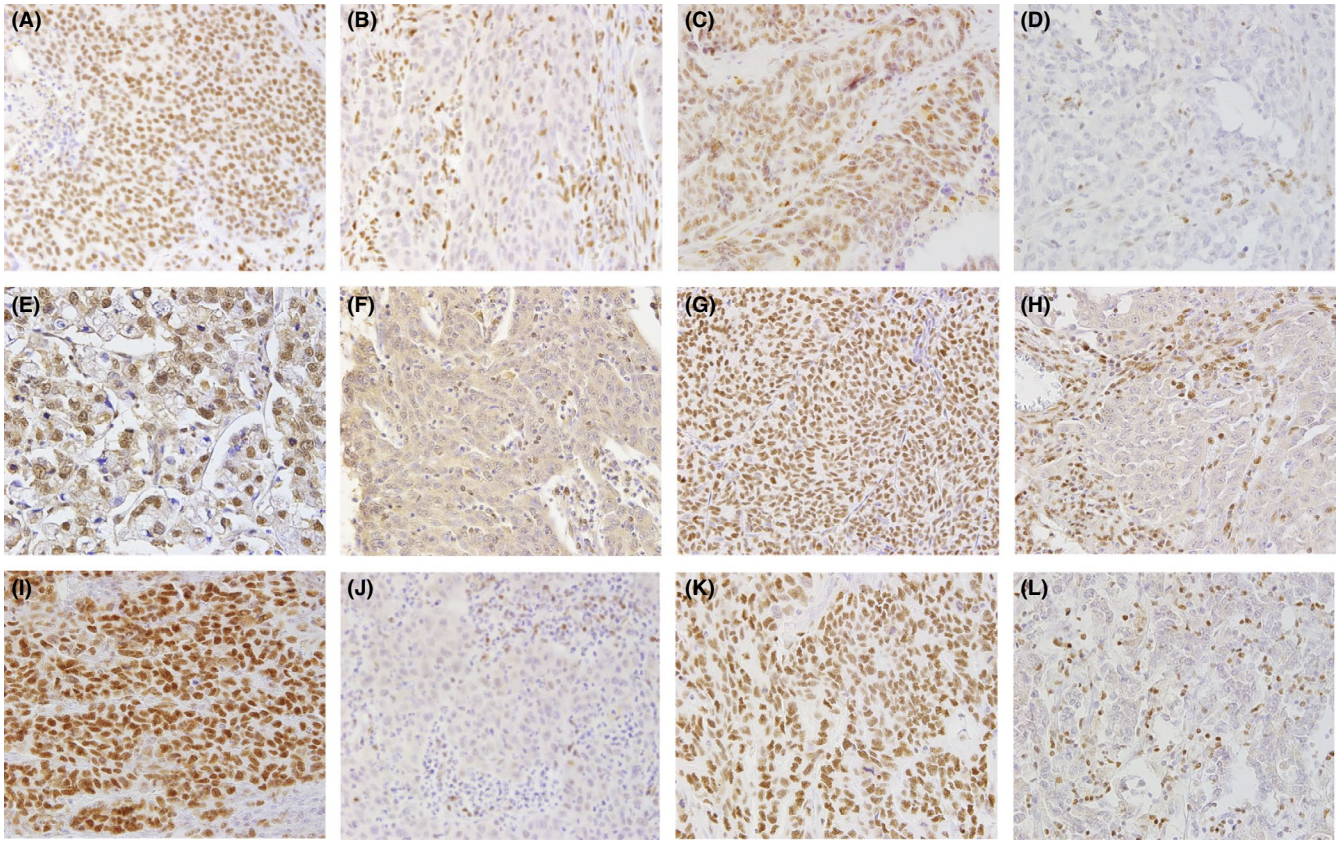

FIGURE 2 Representative immunohistochemical images of ARID1A (A, B), BRG1 (C, D), BRM (E, F), INI1 (G, H), BAF155 (I, J), and BAF170 (K, L) in solid-type poorly differentiated adenocarcinomas. Note the retained expressions of ARID1A (A), BRG1 (C), BRM (E), INI1 (G), BAF155 (I), and BAF170 (K). Note the loss of expression of ARID1A (B), BRG1 (D), BRM (F), INI1 (H), BAF155 (J), and BAF170 (L), whereas lymphocytes, fibrocytes, and vascular endothelial cells show retained expression of SWI/SWF subunits

mutational analyses, respectively, because of an insufficient quality of DNA or level of PCR amplification. *KRAS* mutations at codon 12 (GGT to GAT [Gly to Asp]) were observed in 2 solid-type PDA cases, and *BRAF* mutation at codon 600 of exon 15 (GTG to GAG [Val to Glu]) was observed in 1 solid-type PDA case.

We analyzed the MSI status of 21 MMR-deficient solid-type PDAs to validate the immunohistochemistry of MMR proteins. We excluded 8 tumors because of insufficient quality of DNA or level of PCR amplification. The MSI analysis revealed that all 13 MMR-deficient solid-type PDAs were MSI-High.

3.4 | Prognosis after surgery

The Kaplan-Meier curves illustrating the comparison of solid-type PDAs and GC in the control group, and the association of immunohistochemical status with survival in the solid-type PDA patients are shown in Figure 4. There was no significant difference between the solid-type PDAs and GC in the control group (P = .4282). In the solid-type PDAs, the MMR-deficient group showed relatively longer overall survival than the MMR-proficient group, but the difference did not reach significance (P = .1125). The ARID1A complete/partial loss group showed significantly longer overall survival than the ARID1A retained group (P = .0203). There were no significant correlations between other SWI/SNF subunits and prognosis in solid-type PDAs. As for TNM stage, there were no significant correlations between the expression status of each SWI/SNF complex subunit (retained vs complete/partial loss) and cancer depth (pT1b-2 vs pT3-4) or cancer stage (pStage I/II vs pStage III/IV) (Table 6).

4 | DISCUSSION

We expanded our understanding of the clinicopathological and molecular features of gastric solid-type PDA in the present study. Mismatch repair deficiency was seen in 21 of 54 cases (39%), and all of them showed a concurrent loss of the MLH1/PMS2 pattern. Arai et al reported that the proportion of MSI in solid-type PDA was 43.0%-51.6%,[6,7] which is similar to our present finding. Other studies showed MLH1 loss in GC (16%-19%), complete or partial loss of ARID1A in GC (11%-19%), and complete or partial loss of ARID1A in GC with MLH1 loss (29%-33%).[10,11] Our present analyses revealed much more frequent MMR deficiency in solid-type PDAs (21/54, 39%), complete or partial loss of ARID1A in solid-type PDAs (21/54, 39%), and complete or partial loss of ARID1A in MMR-deficient solid-type PDAs (76%) compared to other histological types of GC in previous studies and the present study.

TABLE 4 Comparison of immunohistochemical status between glandular and solid components

	MMR-deficient group (n = 18)			MMR-proficient group (n = 23)		
	Glandular, n (%)	Solid, n (%)	*P* value	Glandular, n (%)	Solid, n (%)	*P* value
ARID1A						
Complete loss	4 (22)	12 (67)	.0268*	2 (9)	3 (13)	.2966
Partial loss	4 (22)	2 (11)		0 (0)	2 (9)	
Retained	10 (56)	4 (22)		21 (91)	18 (78)	
INI1						
Complete loss	1 (6)	1 (6)	.3456	0 (0)	1 (4)	.312
Partial loss	0 (0)	2 (11)		0 (0)	0 (0)	
Retained	17 (94)	15 (83)		23 (100)	22 (96)	
BRG1						
Complete loss	6 (33)	13 (72)	.0181*	5 (22)	11 (48)	.012*
Partial loss	4 (22)	4 (22)		3 (13)	7 (30)	
Retained	8 (44)	1 (6)		15 (65)	5 (22)	
BRM						
Complete loss	4 (22)	7 (39)	.0224*	6 (26)	9 (39)	.3248
Partial loss	2 (11)	7 (39)		5 (22)	7 (30)	
Retained	12 (67)	4 (22)		12 (52)	7 (30)	
BAF155						
Complete loss	2 (11)	6 (33)	.0071*	0 (0)	0 (0)	.3454
Partial loss	5 (28)	10 (56)		6 (26)	9 (39)	
Retained	11 (61)	4 (22)		17 (74)	14 (61)	
BAF170						
Complete loss	2 (11)	3 (17)	.6299	0 (0)	0 (0)	.321
Partial loss	0 (0)	0 (0)		0 (0)	1 (4)	
Retained	16 (89)	15 (83)		23 (100)	22 (96)	

Note: Data were analyzed using the χ^2 test.

Abbreviation: MMR, mismatch repair.

*Statistically significant.

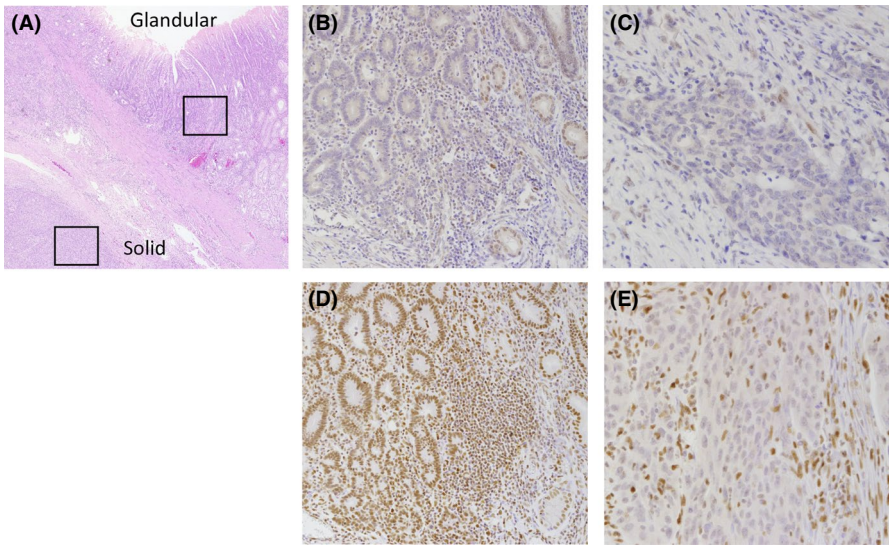

FIGURE 3 A, Mismatch repair-deficient solid-type poorly differentiated adenocarcinoma with a glandular component at the superficial area. B, C, Both the glandular and solid components showed MLH1 loss. D, E, Only the solid component showed a complete loss of ARID1A

The solid-type PDAs often contained a glandular component at the superficial area in both the MMR-deficient group (18/21, 86%) and MMR-proficient group (23/33, 70%), suggesting that most solid-type PDAs developed from differentiated-type adenocarcinomas such as tubular or papillary adenocarcinomas. We observed the loss of SWI/SNF members more frequently in solid components compared

TABLE 5 Result of mutational analysis in solid-type poorly differentiated adenocarcinomas

	All cases	MMR-deficient	MMR-proficient	
	n = 54; n (%)	n = 21; n (%)	n = 33; n (%)	*P* value
KRAS (codons 12 and 13)				
Wild-type	39 (95)	13 (93)	26 (96)	.1597
Mutant-type	2 (5)	1 (7)	1 (4)	
Unknown	13	7	6	
BRAF (V600)				
Wild-type	41 (98)	15 (94)	26 (100)	.1970
Mutant-type	1 (2)	1 (6)	0 (0)	
Unknown	12	5	7	

Note: Data were analyzed using the χ^2 test.
Abbreviation: MMR, mismatch repair.

to glandular components in MMR-deficient and MMR-proficient groups. In the present study, all 21 of the MMR-deficient solid-type PDAs (100%) and 30 of the 33 MMR-proficient solid-type PDAs (91%) showed a complete or partial loss of at least 1 of the SWI/SNF complex subunits. Several studies indicated that the loss of ARID1A or INI1 was associated with medullary morphology in colorectal cancer,[13,14,25,26] and that the loss of BRG1 or BRM was associated with solid morphology in lung cancer.[27] Our present findings suggest that the loss of the SWI/SNF complex plays a role in a morphological shift from glandular to solid component as a second hit rather than carcinogenesis.

It was reported that the loss of BRM or ARID1A in GC was associated with poorly differentiated histology.[11,28] Yan et al reported that ARID1A knockdown in GC cell lines induced a downregulation of E-cadherin transcription and morphological changes of GC cells with increased expressions of mesenchymal markers.[29] Banine et al[30] suggested that the loss of SWI/SNF family members such as BRG1 or BRM induces E-cadherin promoter methylation. These mechanisms could be related to a morphological shift in GC.

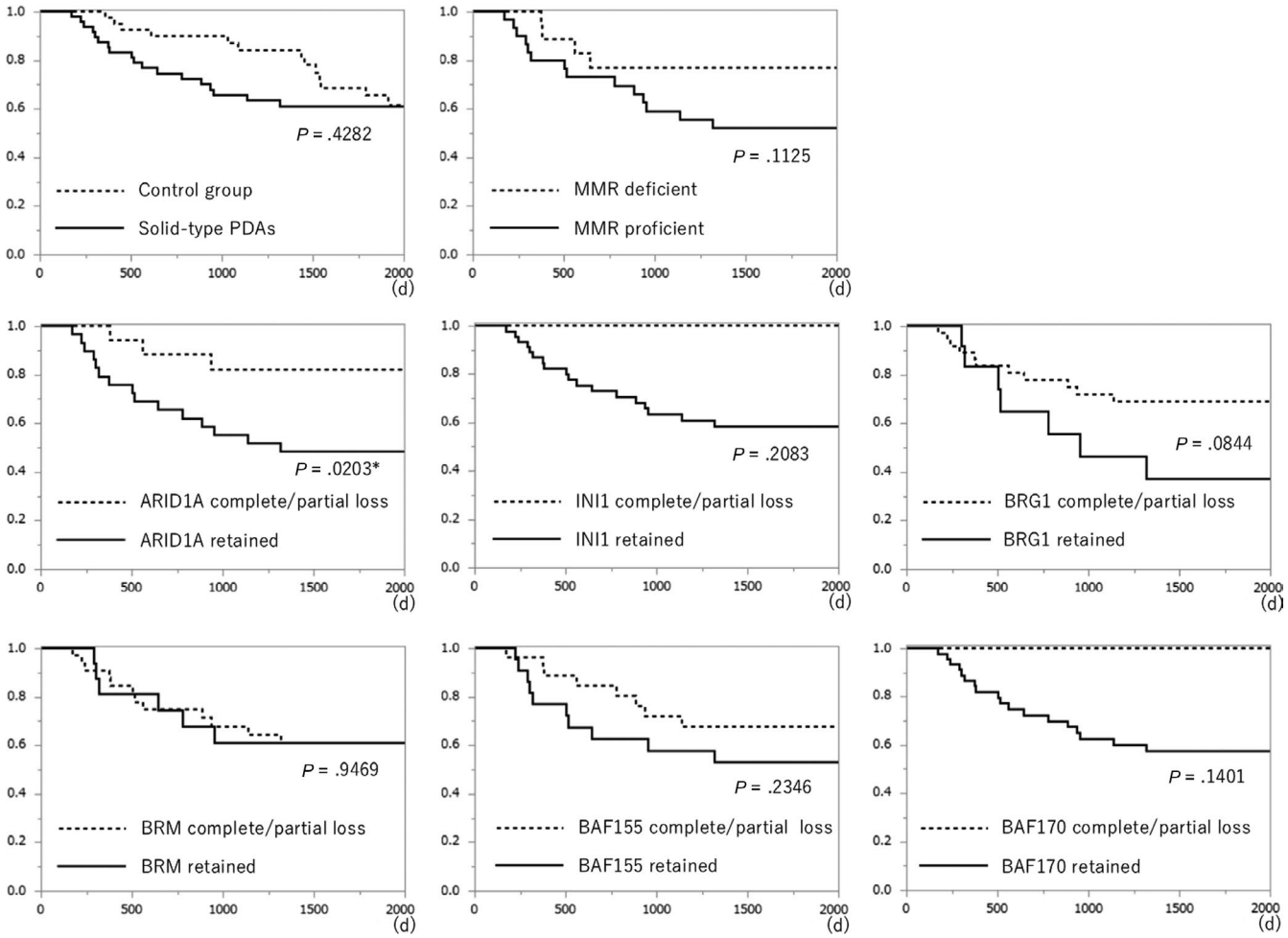

FIGURE 4 Kaplan-Meier curves illustrating the comparison of solid-type poorly differentiated adenocarcinomas (PDAs) and gastric cancers in the control group, and the association of immunohistochemical status with survival in solid-type PDA patients. There was no significant difference between the solid-type PDAs and gastric cancers in the control group (*P* = .4282). In the solid-type PDAs, the mismatch repair (MMR)-deficient group showed relatively longer overall survival than the MMR-proficient group (*P* = .1125). The ARID1A complete/partial loss group showed significantly longer overall survival than the ARID1A retained group (*P* = .0203). There were no significant correlations between other SWI/SNF subunits and prognosis in solid-type PDAs

TABLE 6 Relationship between immunohistochemical status and TNM stage in solid-type poorly differentiated adenocarcinomas

	pT stage			pStage		
	pT1b-2	pT3-4		pStage I/II	pStage III/IV	
	n = 15; n (%)	n = 39; n (%)	*P* value	n = 30; n (%)	n = 24; n (%)	*P* value
ARID1A						
Complete/partial loss	8 (53)	13 (33)	.1769	12 (40)	9 (38)	.8515
Retained	7 (47)	26 (67)		18 (60)	15 (63)	
INI1						
Complete/partial loss	1 (7)	3 (8)	.8974	4 (13)	0 (0)	.063
Retained	14 (93)	36 (92)		26(87)	24 (100)	
BRG1						
Complete/partial loss	11 (73)	31 (79)	.6261	24 (80)	18 (75)	.6605
Retained	4 (27)	8 (21)		6 (20)	6 (25)	
BRM						
Complete/partial loss	11 (73)	25 (64)	.5192	20 (67)	16 (67)	1.0
Retained	4 (27)	14 (36)		10 (33)	8 (33)	
BAF155						
Complete/partial loss	10 (67)	19 (49)	.2361	18 (60)	11 (46)	.2995
Retained	5 (33)	20 (51)		12 (40)	13 (54)	
BAF170						
Complete/partial loss	3 (20)	1 (3)	.0604	4 (13)	0 (0)	.063
Retained	12 (80)	38 (97)		26 (87)	24 (100)	

Note: Data were analyzed using the χ^2 test.

The overwhelming majority of GCs are associated with chronic gastritis by *Helicobacter pylori* infection.[31] Chronic gastritis induces MLH1 promoter methylation,[32] which leads to loss of MLH1 protein and MSI status. In our comparison of the MMR-deficient and MMR-proficient groups, we found that female sex, lower third location, expansive growth pattern, TILs, Crohn's-like reaction, and loss of ARID1A, BRG1, and BAF155 were more frequently present in the MMR-deficient group compared to the MMR-proficient group. The features of the MMR-deficient solid-type PDAs are similar to those of colorectal MC, which is associated with female sex, right-side colon, TILs, Crohn's-like reaction, MSI, favorable prognosis, and ARID1A loss.[24,33-37] These similarities suggest that MMR-deficient solid-type PDA is a gastric counterpart of colorectal MC, as illustrated in Figure 5.

In the MMR-deficient group, we observed the loss of SWI/SNF members (ARID1A, BRG1, BRM, and BAF155) significantly more frequently in solid components compared to glandular components. Only ARID1A loss was associated with favorable prognosis in solid-type PDAs. As discussed already, the features of colorectal MC are ARID1A loss, MSI, and favorable prognosis. Therefore, ARID1A aberration could play a main role in the morphological shift to these histological types, especially in microsatellite unstable tumors of stomach and colon. In the MMR-proficient group, we observed the loss of BRG1 significantly more frequently in solid components compared to glandular components, whereas there were no significant differences of other SWI/SNF complex subunits between solid and glandular components. BRG1 might play a main role in the morphological shift in MMR-proficient solid-type PDAs.

In the present study, we focused on solid-type PDA because of its distinct features, such as a favorable prognosis and high frequency of MSI compared to nonsolid-type PDA.[1,6,7] Solid-type PDA seems to correspond to solid carcinoma, which is a poorly differentiated variant of tubular adenocarcinoma in the WHO classification.[38] Solid carcinoma is similar to intestinal-type GC in molecular features.[39] Nonsolid-type PDA and signet-ring cell carcinoma correspond to diffuse-type GC in Lauren's classification[40] or poorly cohesive carcinoma in the WHO classification.[38]

According to The Cancer Genome Atlas, diffuse-type morphology is associated with GS, which is one of the molecular subtypes of GC.[9] ARID1A alteration is rarer in GS-subtype tumors compared to MSI or EBV subtypes.[9] Additionally, nonsolid-type PDAs and signet-ring cell carcinomas showed rarer losses of SWI/SNF complex subunits than solid-type PDAs in the present study. Therefore, the loss of SWI/SNF family members might induce solid morphology rather than some other poorly differentiated histology.

A previous study reported that ARID1A knockdown promotes tumor growth in xenograft models.[22] In this study, solid-type PDAs showed larger size, more frequent expansive growth, and losses of SWI/SNF family members compared to GC in the control group. However, there were no correlations between the expressions of SWI/SNF complex subunits and cancer depth or cancer stage in solid-type PDAs. Deficiency in any of the SWI/SNF complex subunits

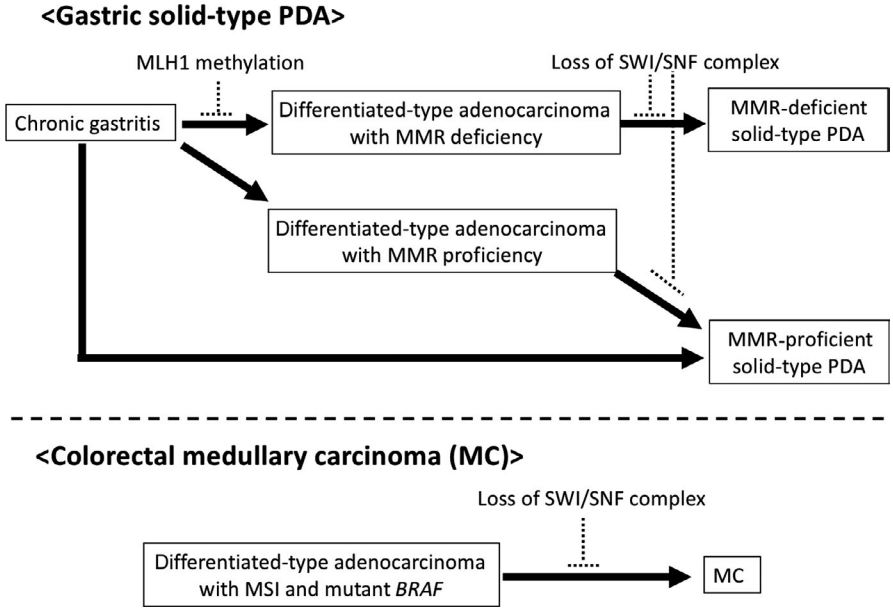

FIGURE 5 Schematic representation of the hypothetical roles of mismatch repair (MMR) and SWI/SNF complex in gastric solid-type poorly differentiated adenocarcinomas (PDAs). The loss of MLH1 due to hypermethylation would lead to microsatellite instability (MSI) status, which promotes carcinogenesis. The loss of SWI/SNF complex family members such as ARID1A would promote a morphological shift as a second hit rather than carcinogenesis. Colorectal medullary carcinoma (MC) is similar to MMR-deficient solid-type PDA except for its high frequency of *BRAF* mutation

did not correlate with unfavorable prognosis. Although deficiency of the SWI/SNF complex could promote expansive growth, it might not contribute to aggressive behavior in GC.

Regarding heterogeneous expressions of SWI/SNF complex subunits, solid-type PDAs often showed different expression patterns of each subunit in solid or glandular components, as discussed above. In addition, some cases labeled "partial loss" of each subunit showed distinctly separated positive expression and negative expression areas in solid components. Previous studies showed intratumoral heterogeneity of SWI/SNF complex subunits in several tumors.[11,22,27] Intratumoral heterogeneity will be an important challenge when the SWI/SNF complex becomes a therapeutic target in the future.

Epstein-Barr virus infection was not frequent (4%) in solid-type PDAs in this study. It was reported that EBVaGC shows a higher density of TILs than GC with MSI.[41] Epstein-Barr virus-associated GC is associated with male sex, upper third location, and lymphoepithelioma-like histology,[42-44] whereas GC with MSI is associated with female sex and lower third location. The clinicopathological features of EBVaGC thus differ from those of MMR-deficient solid-type PDAs.

As for mutational analysis, the frequencies of *BRAF* mutation differ between the gastric solid-type PDAs in our study (2%) and colorectal MCs. Medullary morphology, MSI, and *BRAF* mutation correlate with each other in colorectal cancer,[25,34-37,45] whereas *BRAF* mutation is rare in GC with or without MSI.[9,46,47] These findings suggest that solid-type PDAs are not related to carcinogenesis derived from *BRAF* mutation. As for *KRAS* mutation, van Grieken et al described an association between *KRAS* mutation and MSI in GC,[48] and Arai et al reported relatively frequent *KRAS* mutation (14.1%) in solid-type PDAs. Our finding of a lower *KRAS* mutation rate (5%) is not consistent with these studies. Further examinations of the molecular characteristics of solid-type PDAs are necessary to address this discrepancy.

The present study has several limitations. First, we did not analyze the MSI status of MMR-proficient solid-type PDAs, and MSI analysis failed in several MMR-deficient solid-type PDAs because of poor sample DNA qualities. Second, we did not assess DNA methylation or mutational status of SWI/SNF complex subunits such as ARID1A.

In conclusion, solid-type PDAs showed a frequent loss of MMR proteins and SWI/SNF complex. Our findings also suggest that loss of SWI/SNF complex might induce a morphological shift from differentiated-type adenocarcinoma to solid-type PDA as a second hit rather than carcinogenesis.

ACKNOWLEDGMENTS

We thank all of the technical staff of the Department of Pathology, Kyushu University for their assistance.

DISCLOSURE

The authors declare that there are no conflicts of interest to disclose.

ORCID

Yoshinao Oda https://orcid.org/0000-0001-9636-1182

REFERENCES

1. Kunisaki C, Akiyama H, Nomura M, et al. Clinicopathological properties of poorly-differentiated adenocarcinoma of the stomach: comparison of solid- and non-solid-types. *Anticancer Res*. 2006;26:639-646.
2. Hirai H, Yoshizawa T, Morohashi S, et al. Clinicopathological significance of gastric poorly differentiated medullary carcinoma. *Biomed Res*. 2016;37:77-84.
3. Otsuji E, Kuriu Y, Ichikawa D, et al. Clinicopathologic and prognostic characterization of poorly differentiated medullary-type gastric adenocarcinoma. *World J Surg*. 2004;28:862-865.
4. Lu BJ, Lai M, Cheng L, et al. Gastric medullary carcinoma, a distinct entity associated with microsatellite instability-H, prominent intraepithelial lymphocytes and improved prognosis. *Histopathology*. 2004;45:485-492.
5. Association JGC. Japanese classification of gastric carcinoma. *Gastric Cancer*. 2011;14:101-112.

6. Arai T, Matsuda Y, Aida J, et al. Solid-type poorly differentiated adenocarcinoma of the stomach: clinicopathological and molecular characteristics and histogenesis. *Gastric Cancer*. 2019;22:314-322.
7. Arai T, Sakurai U, Sawabe M, et al. Frequent microsatellite instability in papillary and solid-type, poorly differentiated adenocarcinoma of the stomach. *Gastric Cancer*. 2013;16:505-512.
8. Wang K, Kan J, Yuen ST, et al. Exome sequencing identifies frequent mutation of ARID1A in molecular subtypes of gastric cancer. *Nat Genet*. 2011;43:1219-1223.
9. Cancer Genome Atlas Research Network. Comprehensive molecular characterization of gastric adenocarcinoma. *Nature*. 2014;513:202-209.
10. Abe H, Maeda D, Hino R, et al. ARID1A expression loss in gastric cancer: pathway-dependent roles with and without Epstein-Barr virus infection and microsatellite instability. *Virchows Arch*. 2012;461:367-377.
11. Kim YB, Ham IH, Hur H, et al. Various ARID1A expression patterns and their clinical significance in gastric cancers. *Hum Pathol*. 2016;49:61-70.
12. Jones S, Li M, Parsons DW, et al. Somatic mutations in the chromatin remodeling gene ARID1A occur in several tumor types. *Hum Mutat*. 2012;33:100-103.
13. Ye J, Zhou Y, Weiser MR, et al. Immunohistochemical detection of ARID1A in colorectal carcinoma: loss of staining is associated with sporadic microsatellite unstable tumors with medullary histology and high TNM stage. *Hum Pathol*. 2014;45:2430-2436.
14. Chou A, Toon CW, Clarkson A, et al. Loss of ARID1A expression in colorectal carcinoma is strongly associated with mismatch repair deficiency. *Hum Pathol*. 2014;45:1697-1703.
15. Huang HN, Lin MC, Tseng LH, et al. Ovarian and endometrial endometrioid adenocarcinomas have distinct profiles of microsatellite instability, PTEN expression, and ARID1A expression. *Histopathology*. 2015;66:517-528.
16. Wilson BG, Roberts CW. SWI/SNF nucleosome remodellers and cancer. *Nat Rev Cancer*. 2011;11:481-492.
17. Yaniv M. Chromatin remodeling: from transcription to cancer. *Cancer Genet*. 2014;207:352-357.
18. Kohashi K, Oda Y. Oncogenic roles of SMARCB1/INI1 and its deficient tumors. *Cancer Sci*. 2017;108:547-552.
19. Roberts CW, Orkin SH. The SWI/SNF complex–chromatin and cancer. *Nat Rev Cancer*. 2004;4:133-142.
20. Smyrk TC, Watson P, Kaul K, et al. Tumor-infiltrating lymphocytes are a marker for microsatellite instability in colorectal carcinoma. *Cancer*. 2001;91:2417-2422.
21. Graham DM, Appelman HD. Crohn's-like lymphoid reaction and colorectal carcinoma: a potential histologic prognosticator. *Mod Pathol*. 1990;3:332-335.
22. Jiang W, Dulaimi E, Devarajan K, et al. Immunohistochemistry successfully uncovers intratumoral heterogeneity and widespread colosses of chromatin regulators in clear cell renal cell carcinoma. *PLoS One*. 2016;11(10):e0164554.
23. Fujita K, Yamamoto H, Matsumoto T, et al. Sessile serrated adenoma with early neoplastic progression: a clinicopathologic and molecular study. *Am J Surg Pahol*. 2011;35:295-304.
24. Bando H, Okamoto W, Fukui T, et al. Utility of the quasi-monomorphic variation range in unresectable metastatic colorectal cancer patients. *Cancer Sci*. 2018;109:3411-3415.
25. Pyo JS, Sohn JH, Kang G. Medullary carcinoma in the colorectum: a systematic review and meta-analysis. *Hum Pathol*. 2016;53:91-96.
26. Wang J, Andrici J, Sioson L, et al. Loss of INI1 expression in colorectal carcinoma is associated with high tumor grade, poor survival, BRAFV600E mutation, and mismatch repair deficiency. *Hum Pathol*. 2016;55:83-90.
27. Matsubara D, Kishaba Y, Ishikawa S, et al. Lung cancer with loss of BRG1/BRM, shows epithelial mesenchymal transition phenotype and distinct histologic and genetic features. *Cancer Sci*. 2013;104:266-273.
28. Yamamichi N, Inada K, Ichinose M, et al. Frequent loss of Brm expression in gastric cancer correlates with histologic features and differentiation state. *Cancer Res*. 2007;67:10727-10735.
29. Yan HB, Wang XF, Zhang Q, et al. Reduced expression of the chromatin remodeling gene ARID1A enhances gastric cancer cell migration and invasion via downregulation of E-cadherin transcription. *Carcinogenesis*. 2014;35:867-876.
30. Banine F, Bartlett C, Gunawardena R, et al. SWI/SNF chromatin-remodeling factors induce changes in DNA methylation to promote transcriptional activation. *Cancer Res*. 2005;65:3542-3547.
31. Matsuo T, Ito M, Takata S, et al. Low prevalence of Helicobacter pylori-negative gastric cancer among Japanese. *Helicobacter*. 2011;16:415-419.
32. Alvarez MC, Santos JC, Maniezzo N, et al. MGMT and MLH1 methylation in Helicobacter pylori-infected children and adults. *World J Gastroenterol*. 2013;19:3043-3051.
33. Takahashi S, Kohashi K, Yamamoto H, et al. Expression of adhesion molecules and epithelial-mesenchymal transition factors in medullary carcinoma of the colorectum. *Human Pathol*. 2015;46:1257-1266.
34. Rüschoff J, Dietmaier W, Lüttges J, et al. Poorly differentiated colonic adenocarcinoma, medullary type: clinical, phenotypic, and molecular characteristics. *Am J Pathol*. 1997;150:1815-1825.
35. Knox RD, Luey N, Sioson L, et al. Medullary colorectal carcinoma revised: a clinical and pathological study of 102 cases. *Ann Surg Oncol*. 2015;22:2988-2996.
36. Thirunavukarasu P, Sathaiah M, Singla S, et al. Medullary carcinoma of the large intestine: a population based analysis. *Int J Oncol*. 2010;37:901-907.
37. Friedman K, Brodsky AS, Lu S, et al. Medullary carcinoma of the colon: a distinct morphology reveals a distinctive immunoregulatory microenvironment. *Mod Pathol*. 2016;29:528-541.
38. Lauwers GY, Carneiro F, Graham DY, et al. Gastric carcinoma. In: Bosman FT, Carneiro F, Hruban RH, Theise ND, eds. *WHO classification of tumours of the digestive system*, 4th ed. Lyon, France: WHO Publisher; 2010:48-63.
39. Jiao YF, Sugai T, Habano W, et al. Clinicopathological significance of loss of heterozygosity in intestinal- and solid-type gastric carcinomas: a comprehensive study using the crypt isolation technique. *Mod Pathol*. 2006;19:548-555.
40. Lauren P. The two, histological main types of gastric carcinoma: diffuse and so-called intestinal-type carcinoma. An attempt at a histo-clinical classification. *Acta Pathol Microbiol Scand*. 1965;64:31-49.
41. Chiaravalli AM, Feltri M, Bertolini V, et al. Intratumour T cells, their activation status and survival in gastric carcinomas characterized for microsatellite instability and Epstein-Barr virus infection. *Virchows Arch*. 2006;448:344-353.
42. Park S, Choi MG, Kim KM, et al. Lymphoepithelioma-like carcinoma: a distinct type of gastric cancer. *J Surg Res*. 2015;194:458-463.
43. Gonzalez RS, Cates JMM, Revetta F, et al. Gastric carcinomas with lymphoid stroma: categorization and comparison with solid-type colonic carcinomas. *Am J Clin Pathol*. 2017;148:477-484.
44. Shinozaki-Ushiku A, Kunita A, Isogai M, et al. Profiling of virus-encoded microRNAs in Epstein-Barr virus-associated gastric carcinoma and their roles in gastric carcinogenesis. *J Virol*. 2015;89:5581-5591.
45. Gelsomino F, Barbolini M, Spallanzani A, et al. The evolving role of microsatellite instability in colorectal cancer: a review. *Cancer Treat Rev*. 2016;51:19-26.
46. Corso G, Velho S, Paredes J, et al. Oncogenic mutations in gastric cancer with microsatellite instability. *Eur J Cancer*. 2011;47:443-451.

47. Wu M, Semba S, Oue N, et al. BRAF/K-ras mutation, microsatellite instability, and promoter hypermethylation of hMLH1/MGMT in human gastric carcinomas. *Gastric Cancer*. 2004;7:246-253.
48. van Grieken NC, Aoyama T, Chambers PA, et al. KRAS and BRAF mutations are rare and related to DNA mismatch repair deficiency in gastric cancer from the East and the West: results from a large international multicentre study. *Br J Cancer*. 2013;108:1495-1501.

How to cite this article: Tsuruta S, Kohashi K, Yamada Y, et al. Solid-type poorly differentiated adenocarcinoma of the stomach: Deficiency of mismatch repair and SWI/SNF complex. *Cancer Sci*. 2020;111:1008–1019. https://doi.org/10.1111/cas.14301